

TieBot: Learning to Knot a Tie from Visual Demonstration through a Real-to-Sim-to-Real Approach

Weikun Peng¹, Jun Lv², Yuwei Zeng¹, Haonan Chen³, Siheng Zhao³,
Jichen Sun², Cewu Lu², Lin Shao^{1†}

¹ School of Computing, National University of Singapore

² Department of Computer Science, Shanghai Jiao Tong University

³ Department of Computer Science and Technology, Nanjing University

Abstract: The tie-knotting task is highly challenging due to the tie’s high deformation and long-horizon manipulation actions. This work presents *TieBot*, a Real-to-Sim-to-Real learning from visual demonstration system for the robots to learn to knot a tie. We introduce the Hierarchical Feature Matching approach to estimate a sequence of tie’s meshes from the demonstration video. With these estimated meshes used as subgoals, we first learn a teacher policy using privileged information. Then, we learn a student policy with point cloud observation by imitating teacher policy. Lastly, our pipeline learns a residual policy when the learned policy is applied to real-world execution, mitigating the Sim2Real gap. We demonstrate the effectiveness of *TieBot* in simulation and the real world. In the real-world experiment, a dual-arm robot successfully knots a tie, achieving 50% success rate among 10 trials. Videos can be found on our [website](#).

1 Introduction

Learning cloth manipulation holds great utility across a wide range of applications. One intriguing domain is robotic tie knotting. Service robots must be adept at tasks like aiding the elderly or individuals with disabilities in dressing for certain social events. Teaching robots to knot ties, as a special case of cloth manipulation, typically pushes the limits of robotic cloth manipulation. This offers valuable insights for tie knotting and the broader field of robotic cloth manipulation.

Cloth manipulation presents challenges for robots due to its high-dimensional state and complex dynamics. Extracting and modeling state information are difficult problems. In contrast, humans have accumulated extensive knowledge about cloth manipulation. These priors make learning from demonstration (LfD) a promising direction. LfD empowers a robot to acquire a policy from expert demonstrations, significantly reducing the need to design task-specific reward functions manually. Consequently, LfD stands as a potent and efficient framework for instructing robots in the execution of complex skills.

However, existing LfD methods struggle with tie-knotting tasks. Kinesthetic demonstration or teleoperation suffers from the complexity of tie-knotting tasks. Tie-knotting tasks require bi-manual operations, placing high demand on human operators’ skills and equipment. For instance, Zhang et al use VR headsets for teleoperation [1]. Thus, simple behavior cloning may be significantly labor-intensive. Learning from visual demonstration is usually an easier approach in terms of collecting demonstration data. But this approach also leads to embodiment gaps. Therefore, researchers attempt to find some object-centric representations that robots can utilize to generate correct actions, overcoming embodiment gaps. Several methods attempt to learn a general visual representation of

† Corresponding author e-mail: linshao@nus.edu.sg

some simple pick-place skills via large-scale pre-training on actionless videos [2, 3, 4]. These works present strong generalizations on the learned visual representations, but none of them shows the ability to learn dexterous manipulation skills that can knot a tie. Other methods such as [5, 6, 7, 8] try to leverage object trajectories or keypoints as representations to guide the policy learning. Such representations are indeed sufficient to describe simple object motions but fail to capture the tie’s complex topology and subtle dynamics.

Compared to the existing LfD work mentioned in the previous paragraph, our insight is that mesh is the most suitable representation for tie-knotting tasks and other complex cloth manipulation tasks. It captures accurate geometric structures and physics properties of the tie, which is crucial for tie-knotting tasks. It also disentangles irrelevant information in the visual demonstrations, such as environment background, object colors, and so forth, enabling the learned policy to apply to different test settings. Therefore, we propose a Real-to-Sim-to-Real LfD framework. First, we propose a Hierarchical Feature Matching method to iteratively estimate the tie’s meshes with cloth simulation from the demonstrated video. We use a cloth simulator called *DiffClothAI* [9] that supports intersection-free contact for cloth to maintain the tie’s topological structure during the estimation process. These estimated meshes from the demonstrated video are then used as subgoals. To learn where to grasp the tie and where to pull the tie from point clouds observations in simulation, we adopt a teacher-student training paradigm similar to [10]. Lastly, our pipeline learns a residual policy when applying the policy to real-world settings, mitigating the sim2real gap.



Figure 1: Our proposed *TieBot* performs a tie-knotting task. We leverage cloth simulation to recover the cloth’s state from human demonstration and learn a goal-condition policy to accomplish the tie-knotting task.

In summary, we make the following contributions: 1) We introduced a systematic LfD framework for a dual-arm robot to learn to knot to tie. 2) We proposed a Hierarchical Feature Matching approach to estimate the tie’s mesh with high deformation from the demonstrated RGB-D video using cloth simulation. 3) With estimated meshes as subgoals, we presented a teacher-student training paradigm to learn grasping points and placing points from point cloud observations in simulation. 4) We conduct experiments in simulation and the real-world to demonstrate the effectiveness and advances of our pipeline. To the best of our knowledge, this work is the first effort to develop a robot system, integrating perception, modeling, and robot learning. It successfully complete the tie-knotting task, which is one of the most complex and challenging cloth manipulation tasks.

2 Related Work

2.1 Cloth Manipulation

Previous work mainly addresses short-horizon cloth manipulation tasks that only involve simple pick-place actions. There are several approaches to learning cloth manipulation skills. One approach is using model-free RL or learned dynamics model to learn cloth unfolding, rope rearranging, and dressing assistance tasks on raw sensor input [11, 12, 13, 14, 15]. Other approaches will collect and annotate data from images [16, 17] or generate demonstration trajectories in simulation [18] to

learn policy. Because of the short-horizon and simple actions features of tasks, it’s also possible to infer correct actions from some visual representations, such as flow between current observation and target images [19].

In contrast, tie-knotting tasks require flipping or rotating a part of the tie, which makes it difficult to annotate robot actions or design action primitives. Therefore, collecting and annotating robot actions on observations is infeasible. It’s also difficult to generate demonstrations or directly apply RL in simulation since the trajectories of tie-knotting tasks are much longer and the possible state space is much larger. Thus, in this work, we choose to learn skills from human demonstration.

2.2 Learning from Visual Demonstration

One line of research explores pre-training neural representations from actionless videos [20, 21, 2, 22, 3, 4, 23]. This approach aims at learning general representations for different actions, whereas none of them shows the ability to learn dexterous manipulation skills that can knot a tie. Another line of research attempts to learn from visual priors extracted from visual demonstrations, such as object trajectories [5, 24], hand poses [25, 26], keypoints positions [27, 6], graph relations [7], or affordances [28]. The third approach is to learn a video or trajectory prediction model to guide policy learning [29, 30, 31, 32, 8]. These approaches require in-domain demonstrations, placing restrictions on visual demonstrations. Moreover, the prediction model may suffer from the long-horizon feature of tie-knotting tasks. ORION is the most closely related work, which builds a graph representation from object motions that can generalize across diverse test environments [33]. However, simple graph representations cannot capture the tie’s complex topology and subtle dynamics during the tie-knotting process.

Consequently, we propose explicitly modeling the demonstration as a sequence of meshes. Mesh can accurately describe the tie’s structure and dynamics, which is crucial to learning correct robot actions and generalizing them to different test scenarios.

2.3 Cloth State Estimation

One cloth state estimation method directly predicts cloth states using deep learning [34, 35, 36]. Non-rigid point cloud registration methods such as coherent point drifting are also applied for linear deformable object tracking [37, 38, 39]. However, purely vision-based methods do not guarantee correct cloth topology due to the lack of physics prior. Huang et al. propose a method to reconstruct and track cloth state with a dynamics model [40]. However, this method requires known actions, which cannot be accessed easily from human demonstration sometimes.

Therefore, we propose a Hierarchical Feature Matching method to iteratively estimate the tie mesh in the demonstration video with cloth simulation. Cloth simulation provides important physics prior for state estimation, such as non-penetration, which is crucial for maintaining correct topology.

3 Technical Approach

This work presents a Real-to-Sim-to-Real LfD framework called *TieBot* to guide a dual-arm robot shown in Fig. 1 to knot the tie from an RGB-D demonstration video. An overview of our proposed method is in Fig. 2. We first describe the procedure to estimate the tie’s mesh sequences from the demonstrated video (Sec. 3.1). Using the tie’s mesh sequences as subgoals, we introduce a pipeline to generate robot actions to manipulate the tie, using teacher-student training paradigm (Sec. 3.2). Lastly, we discuss learning residual policy to mitigate Sim2Real gaps (Sec. 3.3).

3.1 Real2Sim

To better estimate the tie’s mesh, we propose to integrate cloth simulation into our pipeline, which provides important physical prior such as non-penetration in the estimation process. We segment the tie in the demonstrated RGB-D video using *Track-Anything* [41] and transform the associated

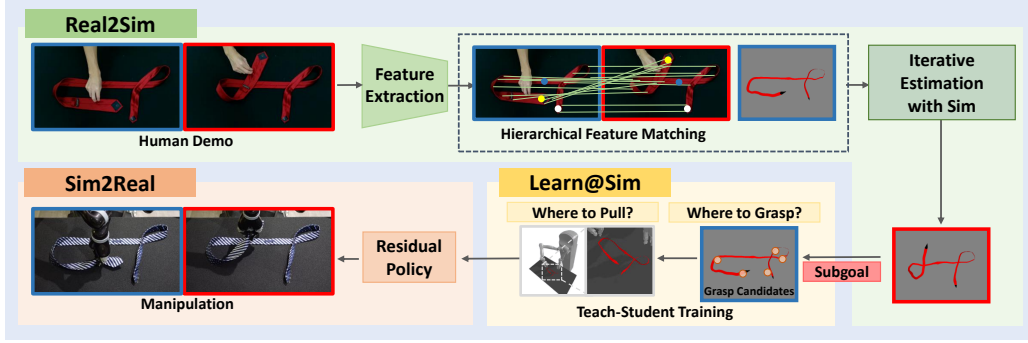


Figure 2: *TieBot* utilizes simulation to estimate the tie’s meshes from the demonstrated video. Then, using mesh sequences as subgoals, we introduce how to generate the robot’s actions to manipulate the tie. The pipeline finally learns a residual policy to reduce the sim2real gap.

segmented depth images into point clouds. Meanwhile, a tie’s mesh is loaded into the *DiffClothAI*. At time step t , we use the tie mesh’s vertices denoted as \mathcal{X}_t^S to describe the tie’s shape. From the RGB images and segmented point clouds denoted as $\{\mathcal{I}_t^D\}$ and $\{\mathcal{X}_t^D\}$, Real2Sim pipeline estimates tie’s mesh sequences $\{\mathcal{X}_t^S\}$ with simulation. The pipeline manually aligns the mesh with the initial frame. We assume the initial mesh fully overlaps with the initial point cloud.

3.1.1 Local Feature Matching

If \mathcal{X}_{t-1}^S and \mathcal{X}_{t-1}^D are aligned and there are correspondences between \mathcal{X}_{t-1}^D and \mathcal{X}_t^D , we can build up the correspondences from the tie’s mesh to the next demonstrated point cloud \mathcal{X}_t^D and move the tie’s vertices to align \mathcal{X}_t^S towards \mathcal{X}_t^D .

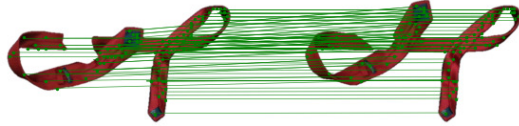


Figure 3: Local Feature matching between two images. A hand caused a gap along the length of the tie during the demonstration.

Here we adopt an off-the-shelf feature matching model called *LoFTR* [42] to build up correspondences between two RGB images \mathcal{I}_{t-1} and \mathcal{I}_t as shown in Fig 3. Typically, *LoFTR* can provide more than a hundred reliable correspondences between two images, which cover almost every visible part of the tie. From the correspondences between \mathcal{I}_{t-1} and \mathcal{I}_t , we can find the feature points on \mathcal{X}_{t-1}^D and their corresponding feature points on \mathcal{X}_t^D . Then, to control the mesh in *DiffClothAI* to align it with \mathcal{X}_t^D , we need to define several vertices on the mesh as control vertices \mathcal{V} . Since \mathcal{X}_{t-1}^S aligns well with \mathcal{X}_{t-1}^D , we map the feature points on \mathcal{X}_{t-1}^D to nearest vertices on \mathcal{X}_{t-1}^S . These vertices are assigned as control vertices \mathcal{V} . Finally, we control \mathcal{V} to move to the positions of feature points on \mathcal{X}_t^D to align \mathcal{X}_t^S towards \mathcal{X}_t^D in *DiffClothAI*.

However, vanilla local feature matching cannot create correspondences in occluded regions, which is common in tie-knotting tasks. We lose the motion information due to occlusion, and the estimation will deviate. Therefore, we propose to add global keypoints information to amend this pipeline.

3.1.2 Keypoints Detection

Keypoints detection can directly build correspondences between mesh vertices and the point cloud. Thus, it will not be affected by occlusion. We define five keypoints along the tie’s surface and the corresponding five key vertices on the mesh, shown in Fig. 4. For each keypoint as the origin, we define the local frame as follows. The z direction is the surface normal

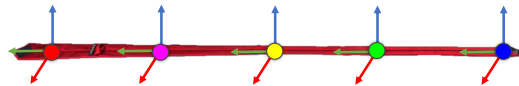


Figure 4: The oriented keypoints to represent the state of the tie. The x,y,z axis are represented by the red, green, blue arrow, respectively.

from the tie’s positive side to the negative side. The x direction is the direction of the tie’s middle skeleton. The y direction is derived using the right-hand rule. These five keypoints, in a predefined order, play the role of the skeleton definition.

Then, we train Pointnet++ [43] to predict the keypoints and associated local frames on the demonstrated point clouds. However, the high-dimensional state makes it challenging to generate sufficient training data to cover all the states encountered in the knotting procedure. A successful tie-knotting trajectory occupies only a small portion of the whole state space of the tie. Thus, uniformly applying random actions on the initial tie’s mesh in the simulation to produce training data fails to cover these states. In contrast, we generate training data based on the current estimated mesh. When we detect the chamfer distance between \mathcal{X}_t^S and \mathcal{X}_t^D is larger than a threshold, we backtrack to the previous time step, gather the tie’s shape \mathcal{X}_{t-1} and apply random actions to the tie’s mesh at $t - 1$ in the simulation to generate annotated training data and train the keypoints prediction network.

3.1.3 Hierarchical Feature Matching(HFM)

Finally, we combine them as Hierarchical Feature Matching(HFM) for state estimation. Control vertices assigned in local feature matching and key vertices will be used together to pull the mesh to target positions specified by local feature matching and keypoints detection. Local feature matching provides detailed motion of vertices, while global keypoints indicate a global tie’s structure. This global structural information ensures the estimation won’t deviate too much, alleviating the shortcomings of the local feature matching method. We use this method to estimate the tie’s meshes from demonstration and output a sequence of meshes $\{\mathcal{X}_t^G\}$. The next part will use these meshes as subgoals to guide robot action generation.

3.2 Learn@Sim

Our pipeline begins to sequentially generate feasible robotic actions in the simulation to guide the tie $\{\mathcal{X}_t^S\}$ towards these subgoals. Since the tie-knotting task is a long-horizon task with multiple grasp and pull actions, we aim to learn where to grasp the tie and where to pull the tie.

For where to pull, we apply a simple strategy. Once we identify the grasping vertices, we pull these vertices to the positions of those vertices on the subgoal. For where to grasp, we adopt a similar teacher-student training paradigm in [10] to ease policy learning. Directly learning from high dimensional observations such as point cloud is data-inefficient because the policy needs to simultaneously learn which features to extract from visual observations and what the high-rewarding actions are. On the contrary, learning a policy via RL from sufficient state information would be much easier, as suggested by [10]. Therefore, we first use privileged information to learn a teacher policy, and then train a student policy imitating teacher policy with point clouds as observations.

Teacher Policy We first learn a teacher policy to select proper grasping points using privileged information. The state s contains the previous tie’s vertices positions and the point-wise displacement for each tie vertices to the subgoal. The action a is one or two grasping vertices of all the tie mesh’s vertices. The reward function \mathcal{R} is defined in equation 1.

Note that we specify the action space as the discrete space (vertex index of the tie). Although there are multiple 6D poses of the robotic grippers to grasp one vertex position of the mesh, the learned policy still reflects the overall grasping quality of these 6D poses associated with one vertex. In the engineering practice, we record each grasping pose offline so that once we figure out the grasping vertices on the tie’s mesh at each timestep, we can automatically produce the feasible grasping poses concerning specific hardware platforms using inverse kinematics.

$$\mathcal{R}(s, a) = \begin{cases} C_1, & \text{if knotting-tie succeeds} \\ -C_2, & \text{if fails to reach any subgoal along the trajectory} \\ C_3 - \|\mathcal{X}_t^S - \mathcal{X}_t^G\|, & \text{Otherwise} \end{cases} \quad (1)$$

For the reward function, here C_1, C_2, C_3 are constant positive values. \mathcal{X}_t^S is the result tie mesh. The failure to reach the subgoal is due to the distance $\|\mathcal{X}_t^S - \mathcal{X}_t^G\|$ is larger than a given threshold, the tie could not be pulled close to the subgoal by grasping on the wrong selected vertex; otherwise, it will return $C_3 - \|\mathcal{X}_t^S - \mathcal{X}_t^G\|$ for intermediate steps or C_1 for the final step.

Student Policy To learn actions from point clouds, we train a student policy to imitate teacher policy. We add some perturbations to the size and positions of the mesh and update the associated trajectories accordingly to generate training data in the simulation. We render point clouds from meshes in PyBullet [44] as the input of our policy network π^{sim} and output the grasping points and placing points positions. We use Pointnet++ [43] as the policy network and train it in a supervised learning manner.

3.3 Sim2Real

When the robot knots the tie in the real world, the robot receives a segmented point cloud of the tie denoted as \mathcal{X}_t^{real} at each time step. Instead of directly applying the action $\pi^{sim}(\mathcal{X}_t^{real})$ in the real world, we train a residual policy that takes in the real point cloud \mathcal{X}_t^{real} and the output of $\pi^{sim}(\mathcal{X}_t^{real})$, outputs small offsets to the positions of predicted grasping points and placing points. Combing the small offsets and predicted grasping and placing points positions, we finally generate the action in real setting. We follow the training process of residual policy described in [45].

4 Experiments

In this section, we introduce our experimental setup and conduct quantitative and qualitative evaluations to demonstrate the effectiveness of our approach. Our experiments focus on answering the following questions.

- How do our pipeline and baseline methods perform on tie-knotting task?
- How does HFM compare to other cloth state estimation methods?
- Can our HFM apply to other cloth manipulation tasks?

Considering the complexity of the entire system, we provide additional experiment results, along with detailed explanations of submodules, in the supplementary materials and [website](#).

4.1 Comparing *TieBot* and baseline

We first evaluate the whole pipeline of *TieBot* and a baseline method in a tie-knotting task. We estimate a sequence of meshes from one human demonstration video. Then, we divide the whole trajectory into 6 parts with 6 subgoals. Our teacher policy learns to select proper grasping points using PPO [46], and student policy imitates the teacher policy to infer grasping points and placing points from the point cloud. We evaluate *TieBot* and the baseline method 10 times for each of the two different ties in *DiffClothAI* and evaluate *TieBot* on two real ties with a dual-arm robot.

Metrics We compare the success rate between our pipeline and ATM [8]. In simulation experiments, if the distance of the final tie’s mesh to the target tie’s mesh is smaller than a threshold, we consider it a success. In real-world experiments, if the little end of the tie is inserted into the hole, as shown in the final stage in Fig. 5, we consider it a success. Since the tie-knotting task is long-horizon, we also compute the averaged number of achieved subgoals for further evaluation.

ATM ATM proposes to model tasks as points trajectories [8]. It first learns a trajectory prediction model, and then learns policy with the learned prediction model using imitation learning. Following similar experiment settings in ATM, we collect 100 demonstration videos in simulation to train the trajectory prediction module. Then, we use the 45 demonstration videos with ground truth action annotations to train the policy network and test the policy in simulation. The action is the 3D offset of the grasping vertices.

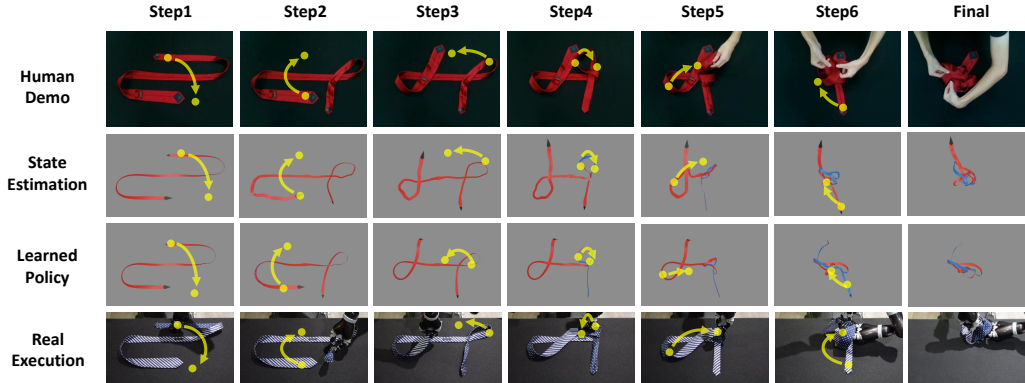


Figure 5: The results of *TieBot* at different stages. We show different sides of the tie in red and blue and manipulation action in yellow to better visualize.

Experiment Result We test *TieBot* on two real ties that differ in materials: one is softer, and the other one is harder. We tested each of them 10 times. We also test *TieBot* and ATM on two ties with different sizes in simulation 10 times for each. The quantitative results are shown in Tab. 1, and qualitative results of

Success Rate / Average Achieved Subgoals	Ours	ATM
normal tie	60% / 5.1	0% / 0.0
larger tie(unseen)	30% / 4.3	0% / 0.0
real tie1(softer)	50% / 5.0	NA / NA
real tie2(harder, unseen)	30% / 4.15	NA / NA

Table 1: Success rate and average achieved subgoals of policy rollouts

TieBot are shown in Fig. 5. This comparison suggests that object trajectories are insufficient to represent subtle dynamics and topology of the tie in tie-knotting tasks. ATM quickly deviates from the correct trajectory since it cannot capture the subtle dynamics of the tie. Therefore, it fails to achieve even one subgoal. This comparison suggests that explicitly modeling the tie in meshes is necessary. For qualitative evaluation, in Fig. 5, we can see that although the tie in the demonstration video, the mesh in the simulation, and the tie used for real robot manipulation are different, our policy can overcome these gaps and learn feasible robot policy.

4.2 Evaluating Hierarchical Feature Matching(HFM)

Real2Sim is the most important part of our pipeline. Without accurate state estimation, particularly estimating the correct topology for the tie, it’s impossible to learn feasible policy to finish the task. To illustrate the importance of different components of HFM and its performance against other cloth state estimation methods, we design three experiments in simulation to test baseline methods and the ablation versions of HFM.

Coherent Point Drift Coherent Point Drift(CPD) is a non-rigid point cloud registration algorithm. We employ the CPD to predict the target positions of the mesh vertices in the target point cloud and directly align the mesh to the target positions.

Ablated Version **Ours w/o KP** stands for only using local feature matching; **Ours w/o LF** stands for using local feature matching and the predicted keypoints positions; **Ours w/o FM** stands for only using predicted keypoints positions and local frames.

Experiment Result The qualitative results are shown in Fig. 6. We can find that either CPD or ablated versions of HFM cannot estimate the target mesh correctly among these three experiments. We also compute the L2 Distance between the vertices of the target mesh and estimated mesh as a quantitative evaluation shown in Tab. 2. It also suggests that the performance will degrade if we cancel some parts of HFM, while CPD deviates a lot from the correct states.

L2 Distance	Ours	Ours w/o FM	Ours w/o KP	Ours w/o LF	CPD
exp1	0.0248	0.0732	0.2424	0.0512	0.1384
exp2	0.0053	0.0107	0.0123	0.0088	0.0661
exp3	0.0032	0.0093	0.0053	0.0049	0.1049

Table 2: Quantitative results of ablation study and comparison to CPD in simulation

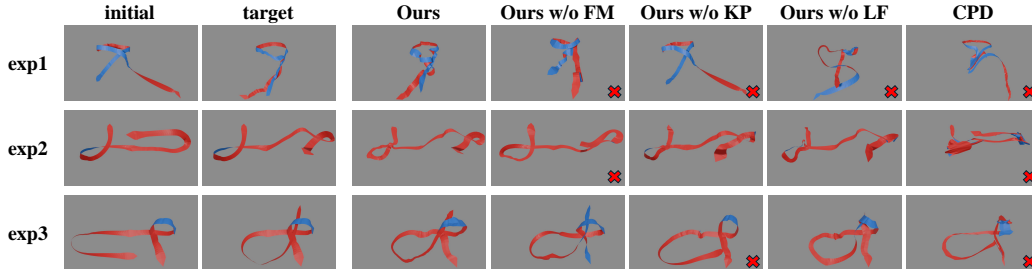


Figure 6: The visualization of the ablation study of HFM in simulation. We put a cross sign in the image’s bottom-right corner to indicate failures of estimating the correct target state, according to human evaluation. Red and blue colors represent different sides of the mesh.

4.3 Apply HFM on Other Cloth Manipulation Tasks

We demonstrate that HFM can be applied to other cloth manipulation tasks. One is a different way to knot a tie. The other one is to fold a towel. We visualize the estimation results in Fig. 7. The results show that HFM can be applied to different cloth manipulation tasks.

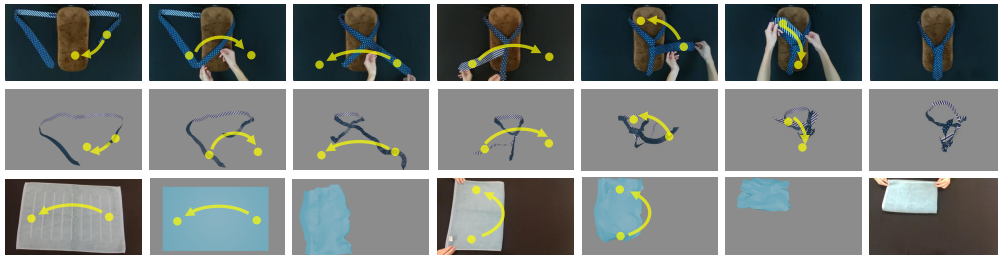


Figure 7: The visualization of a different way to knot a tie and the towel folding. The first row is the human demonstration of tie-knotting, the second row is the estimated states in simulation. While the third row is showing the towel folding. To better visualize, we show the manipulation action in yellow dots and arrows.

5 Conclusion

This work introduces a Real-to-Sim-to-Real LfD framework called *TieBot* for the robots to learn to knot a tie from visual demonstration. *TieBot* introduces the Hierarchical Feature Matching approach to iteratively estimate a sequence of tie’s meshes from the demonstrated video. *TieBot* adopts a teacher-student training paradigm to learn grasping points and placing points from point clouds. Lastly, our pipeline learns a residual policy when the imitated policy is applied to real-world execution, mitigating the Sim2Real gap. We demonstrate that a dual-arm robot successfully knots the tie with our framework, achieving 50% success rate over 10 trials.

Nonetheless, our pipeline has some limitations. First, our pipeline still requires manually setting the initial state of the tie at the beginning of the Real2Sim stage. Second, our Real2Sim module requires training keypoints detection models iteratively, which takes a lot of time. Third, due to the hardware limits, the last step in the real-world experiments shown in Fig. 5 is hardcoded action. Better cloth mesh reconstruction methods, video tracking methods, and more dexterous robot arms may alleviate these issues.

References

- [1] T. Zhang, Z. McCarthy, O. Jow, D. Lee, X. Chen, K. Goldberg, and P. Abbeel. Deep imitation learning for complex manipulation tasks from virtual reality teleoperation. In *2018 IEEE International Conference on Robotics and Automation (ICRA)*, pages 5628–5635, 2018. doi:10.1109/ICRA.2018.8461249.
- [2] S. Nair, A. Rajeswaran, V. Kumar, C. Finn, and A. Gupta. R3m: A universal visual representation for robot manipulation. *arXiv preprint arXiv:2203.12601*, 2022.
- [3] I. Radosavovic, T. Xiao, S. James, P. Abbeel, J. Malik, and T. Darrell. Real-world robot learning with masked visual pre-training. In *Conference on Robot Learning*, pages 416–426. PMLR, 2023.
- [4] K. Shaw, S. Bahl, and D. Pathak. Videodex: Learning dexterity from internet videos. In *Conference on Robot Learning*, pages 654–665. PMLR, 2023.
- [5] D. Seita, Y. Wang, S. Shetty, E. Li, Z. Erickson, and D. Held. ToolFlowNet: Robotic Manipulation with Tools via Predicting Tool Flow from Point Clouds. In *Conference on Robot Learning (CoRL)*, 2022.
- [6] N. Das, S. Bechtler, T. Davchev, D. Jayaraman, A. Rai, and F. Meier. Model-based inverse reinforcement learning from visual demonstrations. In *Conference on Robot Learning*, pages 1930–1942. PMLR, 2021.
- [7] S. Kumar, J. Zamora, N. Hansen, R. Jangir, and X. Wang. Graph inverse reinforcement learning from diverse videos. In *Conference on Robot Learning*, pages 55–66. PMLR, 2023.
- [8] C. Wen, X. Lin, J. So, K. Chen, Q. Dou, Y. Gao, and P. Abbeel. Any-point trajectory modeling for policy learning, 2023.
- [9] X. Yu, S. Zhao, S. Luo, G. Yang, and L. Shao. Diffclothai: Differentiable cloth simulation with intersection-free frictional contact and differentiable two-way coupling with articulated rigid bodies. In *2023 IEEE/RSJ International Conference on Intelligent Robots and Systems (IROS)*. IEEE, 2023.
- [10] T. Chen, M. Tippur, S. Wu, V. Kumar, E. Adelson, and P. Agrawal. Visual dexterity: In-hand reorientation of novel and complex object shapes. *Science Robotics*, 8(84):eadc9244, 2023. doi:10.1126/scirobotics.adc9244. URL <https://www.science.org/doi/abs/10.1126/scirobotics.adc9244>.
- [11] H. Ha and S. Song. Flingbot: The unreasonable effectiveness of dynamic manipulation for cloth unfolding. In *Conference on Robot Learning*, pages 24–33. PMLR, 2022.
- [12] Y. Wu, W. Yan, T. Kurutach, L. Pinto, and P. Abbeel. Learning to manipulate deformable objects without demonstrations. *arXiv preprint arXiv:1910.13439*, 2019.
- [13] Y. Deng, C. Xia, X. Wang, and L. Chen. Deep reinforcement learning based on local gnn for goal-conditioned deformable object rearranging. In *2022 IEEE/RSJ International Conference on Intelligent Robots and Systems (IROS)*, pages 1131–1138. IEEE, 2022.
- [14] Y. Wang, Z. Sun, Z. Erickson, and D. Held. One policy to dress them all: Learning to dress people with diverse poses and garments. In *Robotics: Science and Systems (RSS)*, 2023.
- [15] M. Yan, Y. Zhu, N. Jin, and J. Bohg. Self-supervised learning of state estimation for manipulating deformable linear objects. *IEEE robotics and automation letters*, 5(2):2372–2379, 2020.
- [16] Y. Avigal, L. Berscheid, T. Asfour, T. Kröger, and K. Goldberg. Speedfolding: Learning efficient bimanual folding of garments. In *2022 IEEE/RSJ International Conference on Intelligent Robots and Systems (IROS)*, pages 1–8. IEEE, 2022.

- [17] D. Seita, N. Jamali, M. Laskey, A. K. Tanwani, R. Berenstein, P. Baskaran, S. Iba, J. Canny, and K. Goldberg. Deep transfer learning of pick points on fabric for robot bed-making. In *The International Symposium of Robotics Research*, pages 275–290. Springer, 2019.
- [18] Y. Deng, K. Mo, C. Xia, and X. Wang. Learning language-conditioned deformable object manipulation with graph dynamics. *arXiv preprint arXiv:2303.01310*, 2023.
- [19] T. Weng, S. M. Bajracharya, Y. Wang, K. Agrawal, and D. Held. Fabricflownet: Bimanual cloth manipulation with a flow-based policy. In *Conference on Robot Learning*, pages 192–202. PMLR, 2022.
- [20] P. Sermanet, C. Lynch, Y. Chebotar, J. Hsu, E. Jang, S. Schaal, S. Levine, and G. Brain. Time-contrastive networks: Self-supervised learning from video. In *2018 IEEE International Conference on Robotics and Automation (ICRA)*, pages 1134–1141. IEEE, 2018.
- [21] Y. J. Ma, S. Sodhani, D. Jayaraman, O. Bastani, V. Kumar, and A. Zhang. Vip: Towards universal visual reward and representation via value-implicit pre-training. *arXiv preprint arXiv:2210.00030*, 2022.
- [22] T. Xiao, I. Radosavovic, T. Darrell, and J. Malik. Masked visual pre-training for motor control. *arXiv preprint arXiv:2203.06173*, 2022.
- [23] R. Mendonca, S. Bahl, and D. Pathak. Structured world models from human videos. 2023.
- [24] M. Vecerik, C. Doersch, Y. Yang, T. Davchev, Y. Aytar, G. Zhou, R. Hadsell, L. Agapito, and J. Scholz. Robotap: Tracking arbitrary points for few-shot visual imitation. *arXiv preprint arXiv:2308.15975*, 2023.
- [25] S. Bahl, A. Gupta, and D. Pathak. Human-to-robot imitation in the wild. 2022.
- [26] H. Bharadhwaj, A. Gupta, S. Tulsiani, and V. Kumar. Zero-shot robot manipulation from passive human videos. *arXiv preprint arXiv:2302.02011*, 2023.
- [27] H. Xiong, Q. Li, Y.-C. Chen, H. Bharadhwaj, S. Sinha, and A. Garg. Learning by watching: Physical imitation of manipulation skills from human videos. In *2021 IEEE/RSJ International Conference on Intelligent Robots and Systems (IROS)*, pages 7827–7834. IEEE, 2021.
- [28] S. Bahl, R. Mendonca, L. Chen, U. Jain, and D. Pathak. Affordances from human videos as a versatile representation for robotics. In *Proceedings of the IEEE/CVF Conference on Computer Vision and Pattern Recognition*, pages 13778–13790, 2023.
- [29] K. Schmeckpeper, A. Xie, O. Rybkin, S. Tian, K. Daniilidis, S. Levine, and C. Finn. Learning predictive models from observation and interaction. In *European Conference on Computer Vision*, pages 708–725. Springer, 2020.
- [30] A. Escontrela, A. Adeniji, W. Yan, A. Jain, X. B. Peng, K. Goldberg, Y. Lee, D. Hafner, and P. Abbeel. Video prediction models as rewards for reinforcement learning. *Advances in Neural Information Processing Systems*, 36, 2024.
- [31] Y. Du, S. Yang, B. Dai, H. Dai, O. Nachum, J. Tenenbaum, D. Schuurmans, and P. Abbeel. Learning universal policies via text-guided video generation. *Advances in Neural Information Processing Systems*, 36, 2024.
- [32] P.-C. Ko, J. Mao, Y. Du, S.-H. Sun, and J. B. Tenenbaum. Learning to act from actionless videos through dense correspondences. *arXiv preprint arXiv:2310.08576*, 2023.
- [33] Y. Zhu, A. Lim, P. Stone, and Y. Zhu. Vision-based manipulation from single human video with open-world object graphs. *arXiv preprint arXiv:2405.20321*, 2024.

- [34] C. Chi and S. Song. Garmentnets: Category-level pose estimation for garments via canonical space shape completion. In *Proceedings of the IEEE/CVF International Conference on Computer Vision*, pages 3324–3333, 2021.
- [35] H. Xue, W. Xu, J. Zhang, T. Tang, Y. Li, W. Du, R. Ye, and C. Lu. Garmenttracking: Category-level garment pose tracking. In *Proceedings of the IEEE/CVF Conference on Computer Vision and Pattern Recognition*, pages 21233–21242, 2023.
- [36] Z. Huang, X. Lin, and D. Held. Mesh-based dynamics with occlusion reasoning for cloth manipulation. *arXiv preprint arXiv:2206.02881*, 2022.
- [37] T. Tang, Y. Fan, H.-C. Lin, and M. Tomizuka. State estimation for deformable objects by point registration and dynamic simulation. In *2017 IEEE/RSJ International Conference on Intelligent Robots and Systems (IROS)*, pages 2427–2433. IEEE, 2017.
- [38] T. Tang, C. Wang, and M. Tomizuka. A framework for manipulating deformable linear objects by coherent point drift. *IEEE Robotics and Automation Letters*, 3(4):3426–3433, 2018.
- [39] C. Chi and D. Berenson. Occlusion-robust deformable object tracking without physics simulation. In *2019 IEEE/RSJ International Conference on Intelligent Robots and Systems (IROS)*, pages 6443–6450. IEEE, 2019.
- [40] Z. Huang, X. Lin, and D. Held. Self-supervised cloth reconstruction via action-conditioned cloth tracking. In *2023 IEEE International Conference on Robotics and Automation (ICRA)*, pages 7111–7118. IEEE, 2023.
- [41] J. Yang, M. Gao, Z. Li, S. Gao, F. Wang, and F. Zheng. Track anything: Segment anything meets videos, 2023.
- [42] J. Sun, Z. Shen, Y. Wang, H. Bao, and X. Zhou. LoFTR: Detector-free local feature matching with transformers. *CVPR*, 2021.
- [43] C. R. Qi, L. Yi, H. Su, and L. J. Guibas. Pointnet++: Deep hierarchical feature learning on point sets in a metric space. *arXiv preprint arXiv:1706.02413*, 2017.
- [44] E. Coumans and Y. Bai. Pybullet, a python module for physics simulation for games, robotics and machine learning. <http://pybullet.org>, 2016–2021.
- [45] T. Silver, K. Allen, J. Tenenbaum, and L. Kaelbling. Residual policy learning. *arXiv preprint arXiv:1812.06298*, 2018.
- [46] J. Schulman, F. Wolski, P. Dhariwal, A. Radford, and O. Klimov. Proximal policy optimization algorithms. *arXiv preprint arXiv:1707.06347*, 2017.